RSC Advances

PAPER

View Article Online
View Journal | View Issue

Cite this: *RSC Adv.*, 2020, **10**, 23410

Flexible translucent chitosan–glycerin/QD nanocomposite glue for anti-counterfeiting films with strong adhesion and stability†

Yanyan Chen,* Qi Hu, Qiang Wang, Minghui Yu, Xiaoyu Gong, Shenjie Li,* Jin Xiao, Yingjie Guo, Guangyu Chen and Xinyu Lai

Received 24th March 2020
Accepted 8th June 2020

DOI: 10.1039/d0ra02718a

rsc.li/rsc-advances

With the rapid development of commodity circulation, more attention has been paid to the anticounterfeiting technology of commodities, including stability, universality and ease of distinguishing. The authors report the use of gelatin–chitosan–glycerin/QD nanocomposite-functionalized glue for luminescent anti-counterfeiting labels. As the blend and plasticizer, the addition of chitosan and glycerin effectively improved the flexibility and formability of the gelatin–chitosan–glycerin/QD composite films, which show excellent mechanical properties, including high transparency, luminescence and flexibility, and they are easy to prepare on a large scale, providing certain reference values for new anticounterfeiting technology applying a variety of morphologies.

Introduction

Nanocrystals (NCs) and quantum dots (QDs) with unique photoluminescence and electro-chemical characteristics have played an important role in promoting evolutions in displays, photovoltaic devices and fluorescence label.[1–4] From monochrome display to fingerprint identification, pollutant detection, and fluorescence anti-counterfeiting, QDs' applications are developing towards individualization, microquantification and complication.[5,6] Luminescent QD thin films, with visible fluorescence patterns excited under UV light, possess several potential advantages: small occupation area, no directional constraints, and being easier to read. By combining two wavelength quantum dots with other security technologies, various security functions can be realized, which opens up a new way for security authentication. As most purchasable commodities need to be labeled, such as packaging bags, glasses and corrugated board, possessing diversified irregular shapes and surface features, the required anti-counterfeiting film should meet the requirement of the following characteristics: good flexibility, strong adhesion, and suitable for a variety of materials. As is known, because of their high operability, low cost, and not restricted by the substrates, the glue coating has been successfully applied in the production of thin film solar cells, transistors, and flexible wearable electronic devices,[7–9] which attracted widespread attention as a preferred solution to satisfy the above requirements.

In practical applications, most quantum-dot-based luminescence materials need to stabilize metastable nanoparticles in appropriate substrates, to maintain their initial photo luminescence (PL) efficiency and inhibit their aggregation. Preparing polymer nanocomposites which offer added advantages such as enhanced stability and mechanical properties is the common technology to fabricating the flexible luminescent QDs thin films.[10,11] There are still two issues to be solved: (1) compatibility between QDs and polymers needs to be improved; (2) how to adjust and integrate the properties of QDs and polymers, including mechanical properties and optical properties. In the consideration of environmental friendliness, nature biopolymers, such as cellulose, gelatin and chitosan, are of special interest compared with synthetic polymers.[12] As a kind of eatable organic substance with long-chain, when dissolving in warm water, gelatin can be used as ligands by covering on the surface of quantum dots, which will significantly improve the phenomenon of low quantum efficiency of surface defects caused by the short water-soluble ligand in the preparation of quantum dots in water phase.[13,14] Compared to toxic organic ligands, gelatin coated QDs with high PLQYs can be obtained without polluting the environment as well. Oluwafemi reported gelatin-coated CdTe QDs with high luminescence.[15] However, due to the toxicity of Cd, it is necessary to develop and prepare non-Cd QDs, such as I–III–VI type semiconductors, which are widely considered as the candidate for replacing Cd based luminescent material due to their adjustable band gap by both size and composition.[16–18] Compared with Ag ions, the preparation of Cu-based I–III–VI nanocrystals is more complex because Cu contains two ion states: +1 and +2.

School of Chemistry and Chemical Engineering, Hefei University of Technology, Hefei, Anhui, 230009, People's Republic of China. E-mail: yanyanchen@hfut.edu.cn; shenjieli@hfut.edu.cn

† Electronic supplementary information (ESI) available. See DOI: 10.1039/d0ra02718a

Besides, for Ag and In belong to the same periodic element group, the difference of ion radius between them is small, so people began to pay attention to the preparation of Ag-based I–III–VI NCs. However unfortunately, these fabricated naked I–III–VI QDs exhibited low PLQYs. Compared with the traditional ZnS overcoating methods, introducing Zn into the alloy structure to form I–III–Zn–VI quaternary nanostructure could improving the PL properties (*e.g.*, PLQYs over 70% for quaternary Cu–In–Zn–S QDs[30]) and has received increasing attention.[30–32] Kang *et al.* reported aqueous gelatin coated Ag–In–S QDs gel for white LED by drop-drying method.[19] However, since gelatin is easy to break after drying, it is impossible to prepare flexible films; in addition, the reported range of luminescence is narrow (yellow to orange), which limits the direct preparation of composite white light anticounterfeiting films. As the only natural alkaline polymer, chitosan has been frequently reported as substrate materials for flexible thin films because of its unique qualities with high transparency, good viscosity and film-forming.[20,21] According to Taravel and Domard, glycerine contains abundant hydrophilic hydroxyl groups, which can be cross-linked with gelatin through hydrogen bond and improve the film-forming ability and thin films' tensile strength.[22] By adding chitosan and glycerin to the gelatin-coated QDs solution, it is expected to produce high transparency, flexibility and adhesion glue for the preparation of any form of anti-counterfeiting film. Besides, compared QDs/polyvinyl alcohol (PVA) thin films reported by Pan, the electrophilic activity of amino group is stronger than that of hydroxyl group, and amide bond is more stable than ester bond which promise better physical properties.[23]

In this work, aqueous gelatin-coated high luminescent Ag–In–Zn–S/ZnS QDs with emissions from blue to red region (450–670 nm) are fabricated firstly; the chitosan–glycerin/QDs nanocomposites glue was prepared by adding moderate amount of chitosan and glycerin during physical blending process. Then the novel chitosan–glycerin/QDs nanocomposites thin films (GCG–QDTFs) with high transmittance, flexibility and foldability can be got after drying. It is worth mentioning that considering the QDs solution contains a large number of gelatin as ligands, chitosan can be mixed directly with the crude solution as the blending agent without ligands exchange or removal steps. By controlling the relative content of gelatin–chitosan and glycerin as plasticizer in the GCG–QDTFs, the transmittance, solubility, moisture absorption and mechanical properties were tested respectively to explore the influence of variables on the properties. The properties of the novel quantum-polymer composite anti-counterfeiting film's application on glasses, and plastic bag were further investigated.

Results and discussion

The highly luminescent environment-friendly gelatin-coated Ag–In–Zn–S/ZnS (AIZS/ZnS) core/shell QDs were synthesized in a commercial pressure pot *via* a facile aqueous method. The growth process of NCs varies with time and in this work, the optimum reaction time was confirmed to 60 min as shown in Fig. S1.† The absorption spectra of temporal evolution showed that no change was observed in absorption onset, which indicating that the NCs have already formed in the first 30 min, while the PL intensity reaches to maximum when the reaction time increased from 30 to 60 min. The continuous slightly red-shift of PL peak position indicates that the defects on the crystal surface are increasing while size of the crystal remains the same. This defect states cause the decreasing of PL efficiency can be eliminated by covering a wider band gap semi-conductor to form type-I core/shell heterojunctions. As shown in Fig. S2,† after covering 1 monolayer of ZnS, the PL intensity was improved obviously. Further covering of thicker shell layers will generate the grain boundary splitting and interrupt carrier's path and lead to the decreasing of PL efficiency. Compared to binary QDs, the emission range of multi-component NCs can be adjusted merely by adjusting the ratios of cations, regardless of the size.[24] Since the conduction band (CB) of AIZS core QDs consists of hybrid orbitals of Zn 4s4p and In 5s5p, the increase of In and Zn content will enhance the number of orbitals which improves the conductive band maximum, thus widening the band gap and leading to blue shift of PL peak position. Different starting ratios of AIZS core NCs were fabricated, as shown in Fig. S3A and D,† either increasing the Zn content of Ag : In : Zn $= 1 : 4 : x$ and the In content of Ag : In : Zn $= 1 : x : 1$, both the peak position of PL spectra moved in the short wavelength direction, which is consistent with the blue-shift of band-gap absorption; besides, the same structure information of different component AIZS core NCs also confirmed the formation of quaternary-homogeneous alloy nanocrystals. For the lattice parameters of ZnS NCs is larger than Ag–In–S NCs, the diffraction peak of AIZS shifted to higher angle continuously with the increasing Zn content in AIZS core NCs shown in Fig. S4.† Due to the small sizes of QDs, both the core and core/shell NCs patterns in Fig. 1 got three main broad diffraction peak which can be attributed to the (111), (220), and (311) crystal planes of the NCs in sequence from small to large.[33–35]

Because of the low mismatch between AIZS and ZnS, after covering ZnS shell both peak positions (2θ of 28.6°, 47.5°, 56.3°) and the relative peak intensities of the AIZS/ZnS core/shell

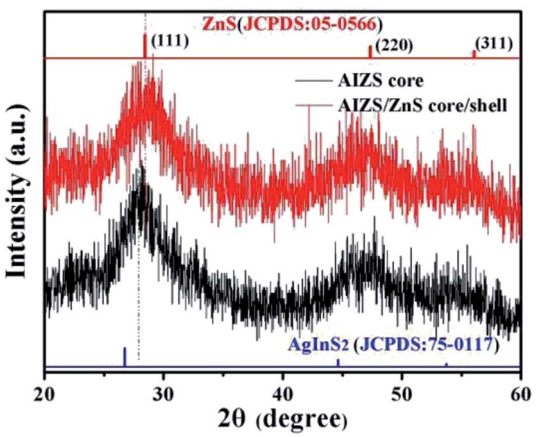

Fig. 1 XRD patterns of AIZS core and 1 monolayer AIZS/ZnS core/shell QDs (Ag : In : Zn = 1 : 4 : 1). Bulk main reflexes for ZnS (JCPDS #05-0566) and $AgInS_2$ (JCPDS #75-0117) are presented by line spectra.

sample with 1 monolayer matched well with the bulk zinc blende ZnS (JCPDS #05-0566). The morphology of AIZS core and AIZS/ZnS core/shell analyzed by TEM is shown in panels A, C and B, D in Fig. 2, both as-prepared core and core/shell NCs have good mono-dispersion and narrow size distribution. After covered 1 monolayer, the clear lattice fringes corresponding to the crystal plane (111) and (220) showed the deposition of ZnS, which is consistent with the data given by XRD diffraction patterns and prove the formation of core/shell structure. The average sizes of the nearly spherical NCs were 2.42 nm and 2.68 nm, respectively. Clear lattice streaks can be seen from the circle, indicating that the QDs has good crystallinity.

The optical properties of QDs, such as the emission range and PLQYs, determined the widely application of QDs thin films. Multi-color emitting light provides more sophisticated anti-counterfeiting features which could accelerate the actual application process of anti-counterfeiting film. In this work, by adjusting the ratios of Ag : In : Zn, broad emission covers 450–680 nm can be obtained directly, corresponding to the red shift of the absorption band edge as the alloying proceeded from 1 : 15 : 29 to 1 : 1 : 0.01. After coating ZnS shell, the PLQY increases from 11.8% to 38.3% in solution (Fig. S5† and 3A). The digital photos in Fig. 3B taken under sunlight and UV-light shows that the QDs solution got high luminescence and transparency which provides guarantee for the preparation of translucent anticounterfeiting film. Besides, since the background will also produce fluorescent signals, which will directly affect the anticounterfeiting material signal, the long fluorescent life is very necessary for anticounterfeiting materials. The fluorescence lifetime calculated from fluorescence decay curves of AIZS/ZnS core/shell QDs (Ag/In/Zn = 1 : 4 : 1) recorded in Fig. S6† exhibited double exponential decay is 628.7 ns, which was consistent with the reported longevity of the I–III–VI based group.[25,26] The long decay time can reduce the possibility of electron–hole recombination, improve the PLQY, and make reading signals of QDs as anti-counterfeiting materials easier.

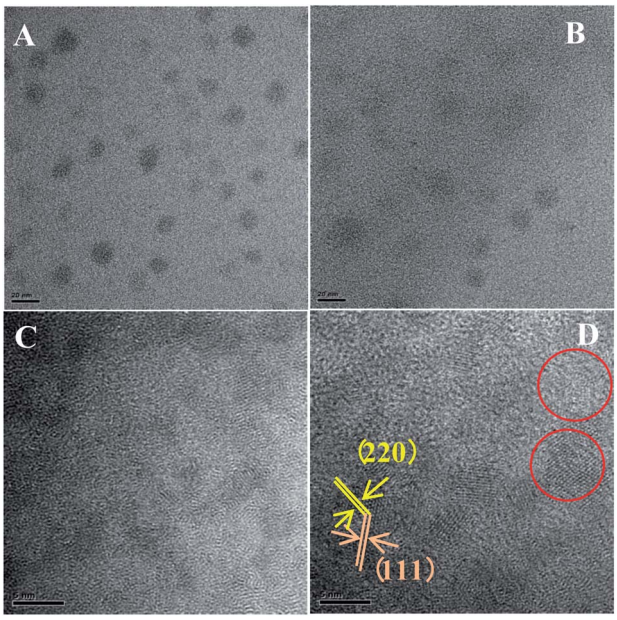

Fig. 2 TEM images of AIZS core (A and C) and 1 monolayer AIZS/ZnS core/shell QDs (B and D) (Ag : In : Zn = 1 : 4 : 1).

Since the lower compatibility between the polymer components of the blend film will generate light scattering, refraction and reflection at the phase interface which thus reducing the transmittance of the film material, the transmittance (*T*%) reflecting the uniformity inside the film becomes an important auxiliary means to determine the compatibility degree of polymer blend film. The transmittance of films in this work with different chitosan/gelatin ratios were recorded, as shown in Table S1.† As the decreasing of chitosan content, the *T*% increasing obviously. Besides, it was found that when the Ch/(Ch + G) ratio was less than 50%, the transparency value was relatively close which indicating that gelatin and chitosan had good compatibility and homogeneity, leading to the high transparency. When the content of chitosan is larger than 50%, the *T*% of the film drops sharply, which is caused by the high degree of crystallinity of chitosan. The *T*% of films with different glycerin/chitosan–gelatin ratios were also investigated and the corresponding *T*% data was shown in Table S2.† It is found that the *T*% of composite films with different glycerine content is relatively high and randomly distributed, indicating the fact that there is no obvious correlation with glycerine amount. The high transmittance also proves that glycerin as plasticizer in the composite film has high compatibility with chitosan and gelatin. Besides, for the actual demand, it is necessary to systematically investigate the mechanical properties of composite flexible films for extensive applications. As shown in Fig. 4A, these stress–strain curves show typical deformation behavior: when given at low strain (<10%), the stress increases rapidly with the increase of strain, and the slope is in the elastic region of the limited elastic modulus; when the strain is higher (>10%), the stress increases slowly until fracture occurs. In particular, with the decrease of chitosan content, the tensile strength of the composite film decreases accompanied by the increasing of the elongation at break, gradually, which is similar to those of composite films prepared with tuna skin or cowhide gelatin and chitosan observed by Gómez-Estaca *et al.*[27] The chitosan component in the blend film belongs to macromolecules with high crystallinity. When the crystallinity is increased, the elastic modulus, strength and stiffness of the material will be improved, which leading to the improvement of the resistance to creep and stress relaxation, coincided with decreasing of the plasticity and impact toughness. This is consistent with our experimental results. Therefore, the strength and flexibility of the composites films can be changed easily by adjusting the ratios of gelatin to chitosan, which according to the two indexes of tensile strength and elongation at break, the ratio of 60Ch : 40G is the better ratio.

For the hydroxyl groups and amino groups of chitosan molecules are easy to interact with carbonyl groups of gelatin molecules by hydrogen bond, which will leading the weaken of the fluidity of the mixed polymer's molecules chain. Besides, the brittle texture, high tensile strength and low breaking elongation is not suitable for fabrication of flexible films. Glycerine with small molecular volume could insert into the

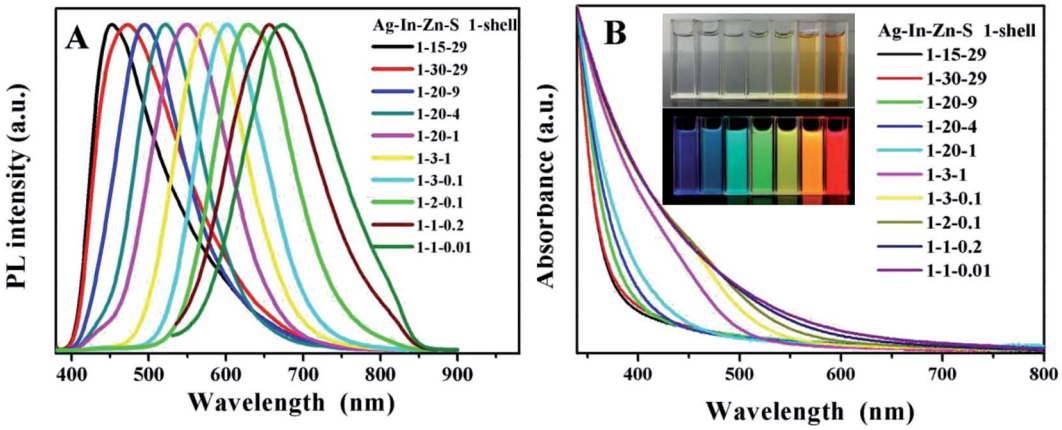

Fig. 3 The fluorescence emission spectra (A) and UV-vis absorption spectra (B) of AIZS/ZnS core/shell QDs with 1 shell obtained under different start ratios and their corresponding digital photos under sunlight (inset) and UV light (inset).

molecular chain and destroy the hydrogen bond, thereby greatly reduce the inter- and intra-molecular forces of the two kinds of polymer, which improved the mechanical properties of the membrane. As shown in Fig. 4C and D, the elongation at break of the composite film increased with the addition of glycerine, while the tensile strength decreased significantly. It is worth mention that when the glycerine content in the films system is very high, the tensile strength of the films will be significantly reduced, and the composite films formed is very sticky, losing its application value. In this paper, the proportion of glycerine content is 10% after comprehensively considering the brittleness and elasticity of the composite films.

It is reported that the water solubility of pure gelatin films is relatively high, about 60%, which restricting the application in wet environment and even water. The adding of chitosan and glycerine both could reduce the water solubility directly, as shown in Fig. S7.† With the increasing of glycerine from 0 to 5%, the water solubility decreased dramatically indicating that the stability of composite films was improved which provided good application conditions.

We also investigated the light transmittance of the composite films prepared by quantum dots emitted by different fluorescence, shown in Table 1. All the thin films with four colors have high transmittance, among which, the composite films prepared by quantum dots emitting green light got the highest light transmittance. The corresponding photos under UV-light and sun light are shown in Fig. 5A and B. The black characters on the background paper can be clearly seen through the mixed film in daylight, indicating that the film has good transparency and smooth surface. Under the excitation of ultraviolet light, we can clearly observe the emission range of quantum dots from blue to red, covering most of the visible region. It is worth mentioning that few films of multiple water-soluble non-cadmium quantum dots can show such high brightness of blue light. By adjusting the Ag/In/Zn ratio, the continuous red shift of the peak value of PL (Fig. 5C) was observed, and the emission of quantum dots within the range of 450 to 656 nm was realized, which was much larger than the range of fluorescence emission reported in other literatures.[28,29] In addition, to demonstrate the flexibility of the mixed film, a picture of crimp of the mixed films is shown in Fig. 5D which shown broad prospects in luminous and display applications.

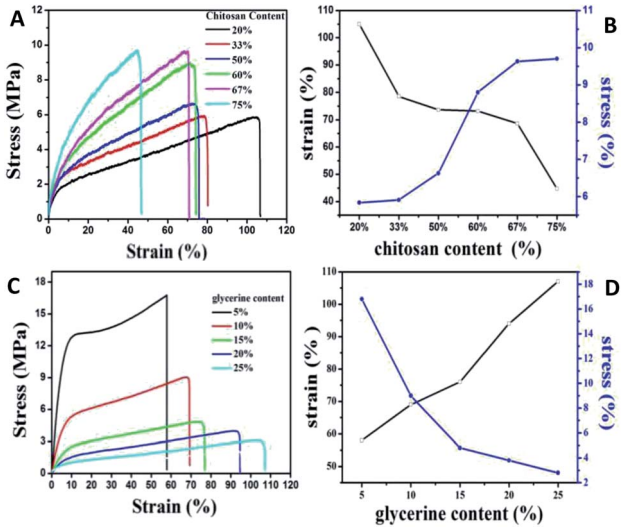

Fig. 4 Typical stress–strain curves (A) and (C) of QDs/gelatin/chitosan hybrid films with different ratios and their corresponding chart of tensile strength and elongation at break (B) and (D).

Table 1 Effect of Ag/In/Zn ratios on transmittance of composite film

	Light transmission (%)	Thickness	Transparency
Samples	600 nm	mm	Value
Orange	85.5	0.0840	0.8099
Yellow	88.6	0.0760	0.6917
Green	89.9	0.0810	0.5709
Blue	87.5	0.0867	0.6689

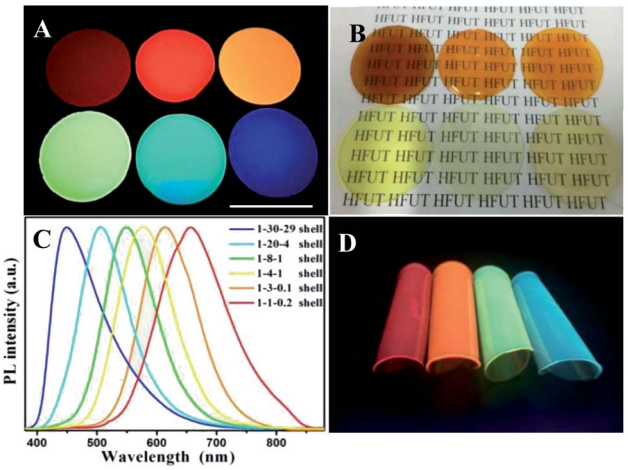

Fig. 5 Digital photos of gelatin–chitosan–glycerin/AgInZnS/ZnS QDs films with G60 : C40 under UV light (A) and visible light (B); (C) corresponding PL spectra of composite films; (D) rolled under UV light.

Further adhesion application of anti-counterfeiting films on glasses, plastic watch dishes and PVC sheets were also investigated. As shown in Fig. S8–S10,† clear patterns can be read under sun light which indicated that all the anti-counterfeiting films fabricated got high transparency. Compared the digital photos taken under UV-light showed the optical performance maintained the same after adding the chitosan and glycerin; besides, except the glasses-samples presented in Fig. S8,† the QDs thin films with gelatin added merely did not attach to the surface of other two substrates (Fig. S9 and S10†) showing poor adhesion. This is even more obvious that the gelatin/QDs thin films (G–QD TFs) break away from PVC sheets after drying without any external force applied, not to mention flexibility. Note that the (a–d) part of G–QD TFs showing in Fig. S10† will crack after drying, while the GCG–QD TFs maintain a good momentum after blending 50 times (Fig. 6A), and no obvious crack can be found in photos taken under UV-light with both core and core/shell NCs (Fig. 6B and C).

The TG curves of the decomposition temperature condition of composite film emitting orange light in Fig. 5D indicates that weight loss is very small (<3.42%) in the range of 50–100 °C, which is water according to the TG and DTG data for the all the initial temperature of thermal decomposition of gelatin, chitosan and glycerin is higher than 117 °C (Fig. S11†). Besides, the three main peaks in DTG curves can be attributed to the thermal decomposition of the three substances which is coincident with Raw feed ratio for preparing films.

As known, the large specific surface area of QDs can be slowly oxidized by air, the oxidation of QDs will lead to the decrease of PLQYs and limit the service time of the films. In our case, QDs were fully covered by a dense and thin gelatin–chitosan–glycerin layer, which can effectively prevent oxidation and aggregation of QDs. After 2 months of air storage, the PLQYs of GCG–QD TFs on glasses shows no decrease, with no obvious absorption intensity increase, as presented in Fig. S12.† Note that the GCG–QD TFs still got strong adhesion and attached over the inner wall of the beaker after the beaker is broken. The strong adhesion and stability could provide certain practical significance in the actual application of anti-counterfeiting films.

Experimental

Materials

Silver nitrate, indium hydroxide, zinc acetate dihydrate, sodium sulfide nonahydrate, thiohydracrylic acid (MPA), thiourea, gelatin (pharmaceutical grade, ~240 g Bloom) and chitosan (deacetylation degreed ≥95%, 100–200 mPa s) were purchased from Aladdin. Isopropanol, glacial acetic acid, ammonia solution ($NH_3 \cdot H_2O$, A.R.) and glycerine were supplied by Tianjin Damao Chemical Reagent Factory. All the initial chemicals in this work were used without further purification.

Synthesis of Ag–In–Zn–S (AIZS) QDs

AIZS cores were synthesized according to our previous report, with some minor modification. In a typical synthesis of AIZS core with Ag/In/Zn ratio of 1 : 4 : 1, 2.4 g of gelatin was added and dissolved in a beaker after adding 80 mL deionized warm water under stirring, followed by adding 800 μL $AgNO_3$ (0.1 mol L^{-1}), 800 μL $Zn(OAc)_2$ (0.1 mol L^{-1}), 2.0 mL $In(OH)_3$ (0.16 mol L^{-1}, 0.2653 g $In(OH)_3$ powder dissolved in 7.77 mL deionized water containing 1.115 mL MPA and 1.115 mL $NH_3 \cdot H_2O$) (the gelatin concentration in solution is ~3% (w/v)). Afterwards, 600 μL Na_2S (1.0 mol L^{-1}) was swiftly injected into the above mixture solution under strong magnetic stirring for 10 min. Subsequently, seal the beaker with plastic wrap and tape, then place the beaker in a commercial electric pressure cooker to heat and pressurize for 50 minutes. AIZS core QDs with starting Ag/In/Zn ratios of 1 : 30 : 39, 1 : 20 : 4, 1 : 2.5 : 0.05 were prepared in the same way as above except for using different amounts of cations.

After 50 minutes, another 2.4 g gelatin, 4.8 mL $Zn(OAc)_2$ (0.1 mol L^{-1}), 960 μL thiourea (1.0 mol L^{-1}) were added in the above crude solution in order under stirring until the gelatin is completely dissolved after the temperature cool to 75 °C (the gelatin concentration in solution is ~6% (w/v)). The reaction will be last for another 50 minutes in the process of ZnS shells' deposition. Note that, the amount of Zn is equally to the total amount of Ag, In, and Zn in the core QDs, which is to obtain a monolayer of ZnS shell. Finally, the core/shell crude solution was stored directly for the fabrication of chitosan–glycerin/QDs nanocomposites glue after cooling down naturally.

Fabrication of chitosan–glycerin/QDs nanocomposites glue and thin films

3.6 mL of AIZS/ZnS core/shell solution was transferred into a 25 mL beaker, followed by adding 2.4 mL chitosan (3% w/v, dissolved in glacial acetic acid) and a mount of glycerin under stirring until the glue is well mixed. The glycerin's content is 5%, 10%, 15%, 20%, 25%, 30% of the total mass of gelatin and chitosan, respectively. The glue was then placed in a 40 °C bath for 30 minutes to debubble, followed by transferring into water-glass (d = 5.5 cm) labelled as 1–6, which was placed in the open air and dried for 3 days.

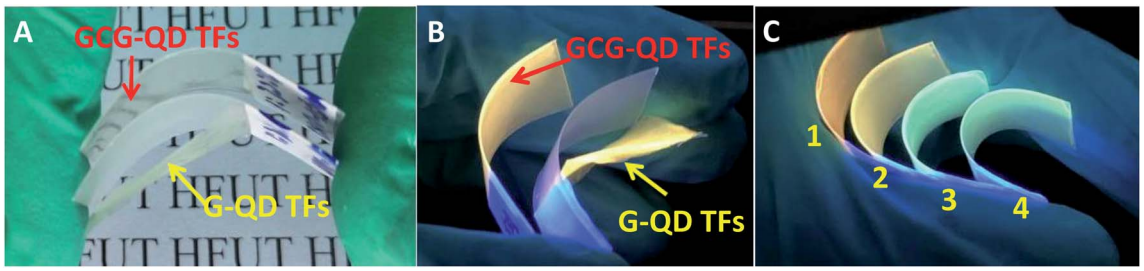

Fig. 6 Digital photographs of curving gelatin/QDs thin films (G–QDTFs) and gelatin–chitosan–glycerin/QDs thin films (GCG–QD TFs) on PVC sheet taken under sunlight (A) and UV-light (B). Part (C) shows curving GCG–QD TFs on PVC sheet (sample 1 to 4 represents the films (e to h) in Fig. S10,† respectively).

Characterizaions

The X-ray diffraction (XRD) measurements were performed on a D8 Focus diffractometer (Bruker) with Cu Kα radiation (λ = 0.15405 nm). Transmission electron microscopy (TEM) was performed using FEI Tecnai G2 S-Twin with a field emission gun operating at 200 kV. Thermogravimetric and differential scanning calorimetry (TG-DSC) data were recorded with a Netzsch Thermoanalyzer STA 409 with a heating rate of 10 °C min^{-1} in N_2 environment. UV-vis absorption spectra were measured by Beijing Pushi General Instrument Tu-1901. The PL measurements were performed with a Hitachi F-7000 spectrophotometer equipped with a 150 W xenon lamp as the excitation source. The mechanical properties of the film are tested by Universal testing machine (UTM4104). The luminescence decay curves were obtained from a Lecroy Wave Runner 6100 digital oscilloscope (1 GHz) using a tunable laser (pulse width = 4 ns, gate = 50 ns) as the excitation source (Continuum Sunlite OPO). The thickness of gelatin films was measured by a step profiler (AMBIOS, XP-100). The Fourier transform infrared (FTIR) spectra were recorded on a Nicolet 6700 spectrophotometer (USA) in the range of 4000–400 cm^{-1}.

Conclusions

In conclusion, we firstly fabricate gelatin–chitosan–glycerin glue blending of AIZS/ZnS core/shell QDs; the flexible translucent thin films got after the glue drying show high luminescence and good film-forming, with adjustable mechanical properties through tuning the ratios of component. Additionally, the concentration of glycerin in the glue can also control the adhesion and stability on both PVC and glass substrates, which is important for solution-based, large-scale, shape-tunable luminescent materials and demonstrates an example for anti-counterfeiting applications.

Conflicts of interest

There are no conflicts to declare.

Acknowledgements

This work is supported by National Natural Science Foundation of China (Grant No. 51502070), Natural Science Foundation of Anhui Province of China (Grant No. 1808085ME111), the Fundamental Research Funds for the Central Universities (Grant No. JZ2018YYPY0307 and JZ2019YYPY0032), and Undergraduate Innovation and Entrepreneurship Training Program (Grant No. S202010359350, S202010359349, X202010359593).

References

1 H. B. Li, K. F. Wu, J. Lim, H. j. Song and V. I. Klimov, *Nat. Energy*, 2016, **1**, 16157.
2 X. M. Li, Y. Wu, S. L. Zhang, B. Cai, Y. Gu, J. Z. Song and H. B. Zeng, *Adv. Funct. Mater.*, 2016, **26**, 2435–2445.
3 Y. Z. Li, P. H. He, S. T. Chen, L. F. Lan, X. Q. Dai and J. B. Peng, *ACS Appl. Mater. Interfaces*, 2019, **11**, 28052–28059.
4 J. H. Liu, L. Cao, G. E. LeCroy, P. Wang, M. J. Meziani, Y. Y. Dong, Y. F. Liu, P. G. Luo and Y. P. Sun, *ACS Appl. Mater. Interfaces*, 2015, **7**, 19439–19445.
5 X. L. Dai, Y. Z. Deng, X. G. Peng and Y. Z. Jin, *Adv. Mater.*, 2017, **29**, 1607002.
6 S. S. Chopra, Y. Q. Bi, F. C. Brown, T. L. Theis, K. Hristovski and P. Westerhoff, *Environ. Sci.: Nano*, 2019, **6**, 3256–3267.
7 Y. H. Chiang, K. Y. Lin, Y. H. Chen, K. Waki, M. A. Abate, J. C. Jiang and J. Y. Chang, *J. Mater. Chem. A*, 2018, **6**, 9629–9641.
8 A. Liu, H. H. Zhu, W. T. Park, S. J. Kang, Y. Xu, M. G. Kim and Y. Y. Noh, *Adv. Mater.*, 2018, **30**, 1802379.
9 D. Kim, Y. Fu, S. Kim, W. Lee, K. H. Lee, H. K. Chung, H. J. Lee, H. Yang and H. Chae, *ACS Nano*, 2017, **11**, 1982–1990.
10 X. B. Wang, W. W. Li and K. Sun, *J. Mater. Chem.*, 2011, **21**, 8558–8565.
11 A. Cosgun, R. L. Fu, W. N. Jiang, J. H. Li, J. Z. Song, X. H. Song and H. B. Zeng, *J. Mater. Chem. C*, 2015, **3**, 257–264.
12 K. Goda, M. S. Sreekala, S. K. Malhotra, K. Joseph and S. Thomas, *Polym. Compos.*, 2013, 1–10.
13 R. Hardman, *Environ. Health Perspect.*, 2006, **114**, 165–172.
14 Y. Y. Chen, S. J. Li, L. J. Huang and D. C. Pan, *Inorg. Chem.*, 2013, **52**, 7819–7821.
15 S. Parani, K. Pandian and O. S. Oluwafemi, *Int. J. Biol. Macromol.*, 2018, **107**, 635–641.
16 H. Z. Zhong, Z. L. Bai and B. S. Zou, *J. Phys. Chem. Lett.*, 2012, **3**, 3167–3175.

17 B. K. Chen, N. Pradhan and H. Z. Zhong, *J. Phys. Chem. Lett.*, 2018, **9**, 435–445.
18 J. Kolny-Olesiak and H. Weller, *ACS Appl. Mater. Interfaces*, 2013, **5**, 12221–12237.
19 X. J. Kang, Y. Y. Chun, L. Wang, S. Wei and D. C. Pan, *ACS Appl. Mater. Interfaces*, 2015, **7**, 27713–27719.
20 J. J. Li, Y. P. Chen, Y. J. Yin, F. L. Yao and K. D. Yao, *Biomaterials*, 2007, **28**, 781–790.
21 S. F. Hosseini, M. Razaei, M. Zandi and F. F. Ghavi, *Food Chem.*, 2013, **136**, 1490–1495.
22 M. N. Taravel and A. Domard, *Biomaterials*, 1996, **17**, 451–455.
23 L. Wang, X. J. Kang and D. C. Pan, *Phys. Chem. Chem. Phys.*, 2016, **18**, 31634–31639.
24 H. J. Zhang and X. Q. He, *Inorg. Chem.*, 2011, **50**, 11958–11964.
25 D. W. Deng, J. Cao, L. Z. Qu, S. Achilefu and Y. Q. Gu, *Phys. Chem. Chem. Phys.*, 2013, **15**, 5078.
26 X. S. Tang, Z. G. Zang, Z. Q. Zu, W. W. Chen, Y. Liu, G. Q. Han, X. H. Lei, X. M. Liu, X. Q. Du, W. M. Chen, Y. Wang and J. M. Xue, *Nanoscale*, 2014, **6**, 11803.
27 J. Gómez-Estaca, M. C. Gómez-Guillén, F. Fernández-Martín and P. Montero, *Food Hydrocolloids*, 2011, **25**, 1461–1469.
28 M. D. Regulacio, K. Y. Win, S. L. Lo, S.-Y. Zhang, X. H. Zhang, S. Wang, M.-Y. Han and Y. G. Zheng, *Nanoscale*, 2013, **5**, 2322.
29 Z. Zang, X. Zeng, M. Wang, W. Hu, C. Liu and X. Tang, *Sens. Actuators, B*, 2017, **252**, 1179–1186.
30 J. Zhang, R. G. Xie and W. S. Yang, *Chem. Mater.*, 2011, **23**, 3357–3361.
31 G. Manna, S. Jana, R. Bose and N. Pradhan, *J. Phys. Chem. Lett.*, 2012, **3**, 2528–2534.
32 B. Zhang, Y. Wang, C. Yang, S. Hu, Y. Gao, Y. Zhang, Y. Wang, H. V. Demir, L. Liu and K. Yong, *Phys. Chem. Chem. Phys.*, 2015, **17**, 25133–25141.
33 T. J. Macdonald, Y. J. Mange, M. Dewi, A. McFadden, W. M. Skinner and T. Nann, *CrystEngComm*, 2014, **16**, 9455–9460.
34 L. Jia, Y. Wang, Q. Nie, B. Liu, E. Liu, X. Hu and J. Fan, *Mater. Lett.*, 2017, **200**, 27–30.
35 W. Guo, W. Yang, Y. Wang, X. Sun, Z. Liu, B. Zhang, J. Chang and X. Chen, *Nano Res.*, 2014, **7**, 1581–1589.